Magneto-thermopower of single-crystal MgB$_2$: Evidence for strong electron-phonon coupling anisotropy

T. Plackowski,[1,*] C. Sułkowski,[1] J. Karpinski,[2] J. Jun,[2] and S. M. Kazakov[2]

[1]*Institute of Low Temperature and Structure Research, Polish Academy of Sciences, ul. Okòlna 2, 50-422 Wrocław, Poland*
[2]*Solid State Physics Laboratory ETH, 8093 Zürich, Switzerland*

The thermoelectric power of superconducting MgB$_2$ single crystals was measured in the temperature range 4–300 K and in a magnetic field up to 13 T. Both the in-plane (S_{ab}) and out-of-plane (S_c) thermopowers was found to be positive, with similar, metal-like temperature dependences and an anisotropy ratio S_{ab}/S_c of the order of 3–4 in the whole temperature range. Unexpectedly low values of S_c were qualitatively explained by the properties of the Fermi surface topology. The analysis of the low temperature ($T<40$ K), normal-state thermopower measured in the magnetic field indicated a domination of the phonon-drag thermopower over the diffusive contribution and gave evidence of a strong (by a factor of 7 ± 1) anisotropy of the electron-phonon coupling. The positive magnetothermopower found above T_c for both directions as well as a negative feature in $S_c(T)$ at $T\sim27$ K for $B>2T$ were tentatively attributed to phonon-drag effects.

I. INTRODUCTION

Since the discovery of the superconductivity in MgB$_2$ at remarkable high value of $T_c=39$ K,[1] a renewed interest has been sparked to the superconducting and normal-state properties of the non-oxide superconductors. This interest was further escalated by the revelation that an anisotropic, complex Fermi surface of MgB$_2$ gives rise to an existence of two distinct superconducting gaps connected with the two different Fermi surface sheets. On the other hand, MgB$_2$ is not as far from conventional superconductors as the high-T_c cuprates are. The pairing symmetry is s,[2] the driving force is the electron-phonon interaction.[3,4] The differences stem mainly from the fact that the charge carriers in MgB$_2$ fall into two distinctive groups: p electrons, similar to those in graphite; and s electrons, which represent highly unusual case of covalent bands crossing the Fermi level. This leads to a complex and uncommon features in the band structure, transport properties and superconductivity.[5] Resistivity measurements for MgB$_2$ show a low residual resistivity of 0.4 mΩ cm and resistivity ratio $R_{300}/R_{4.2}$ values in excess of 20 although the intermetalic compound electron-phonon coupling is apparently large.[6] The resistivity of MgB$_2$ single crystals has been found to be anisotropic with a resistivity ratio of $\rho_c/\rho_{ab}\approx3.5$.[7] The Hall effect with magnetic field parallel to the ab plane is negative (electronlike) in contrast to its positive (holelike) sign with a field parallel to the c axis, indicating presence of both types of charge carriers and, thus, the multiband electronic structure of MgB$_2$.[7]

In this work we present measurements of the magneto-thermopower of the MgB$_2$ single crystals in the temperature range 4–300 K and in the magnetic field up to 13 T. Due to small sizes of the available samples a special procedure has been developed to determine an actual temperature difference across the sample clamped between two Cu blocks. The measurements were performed at configurations with both magnetic field and temperature gradient aligned along two principal crystallographic directions of the MgB$_2$ structure: ab plane and c axis, as well as at a skewed configuration, with $\angle(B,ab)\approx30°$ and $\nabla T\|ab$ plane.

II. EXPERIMENT

Single crystals of MgB$_2$ were grown using with a cubic anvil high pressure technique.[8] All samples were of $\sim0.5\times0.5$-mm area and of ~0.1-mm thickness. Magnetization measurements in $H=2$ Oe performed on three samples selected for thermoelectric power TEP measurements have shown that their properties varied in narrow ranges: transition temperature $T_{c,onset}=38.1$–38.8 K, transition widths $\Delta T_{c,ZFC}=0.65$–1.1 K, and $\Delta T_{c,FC}=1.0$–1.6 K and the ratio between field cooling and zero-field cooling signals FC/ZFC$=0.42-0.69$.

Thermoelectric power (TEP) measurements were carried using two separate equipments. Initial experiments on all single crystals were performed without magnetic field in the temperature range 15–300 K by a steady-state-mode, semi-automatic instrument fitted in the transport liquid helium dewar. One of the samples was further investigated by a fully automatic system working in an Oxford 13/15 T superconducting magnet in the temperature range 1.5–300 K. In this system all measurements were performed upon a slow temperature drift (0.25 K/min).

In both equipments the sample was clamped between two spring-loaded Cu blocks provided with heaters and a pair of thermometers (see Fig. 1). Each thermometer pair was carefully calibrated being glued together (Pt-1000's for semi-automatic equipment and Cernoxes 1050 for the automatic one) to limit an error in the determination of small temperature differences. The blocks were thermally insulated from the surrounding, therefore a thermal difference of any sign might be produced by the heaters. The quality of the thermal contact between the sample and the Cu blocks was tested by electrical resistance measurements, only values below 2 Ω were accepted. The voltage difference between blocks was measured using a A20 (EM Electronics) low-noise preamplifier.
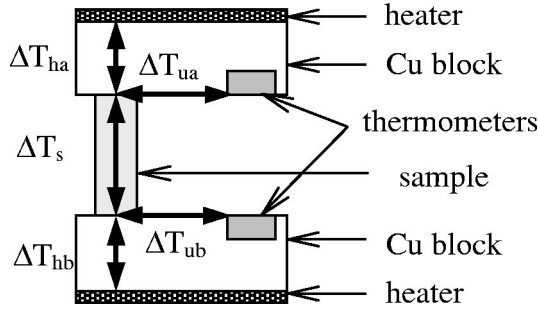
FIG. 1. A setup for thermoelectric power measurements.

A zero-field calibration of both equipments was performed versus a Pb (6N) sample.[9] Since at low temperature the TEP of copper depends strongly on magnetic field[10] and on the material quality[11,12] an additional calibration was necessary for the automatic equipment. This was performed versus a superconducting, optimally doped, polycrystalline $YBa_2Cu_3O_{7-\delta}$ sample with $T_c = 92$ K ($T_c = 76$ K at $B = 13$ T) at fields $B = 0$, 2, 4, 6, 8, 10, and 13 T. The obtained calibration curves were extrapolated up to 100 K.

Another experimental problem was connected with the determination of the actual temperature difference across the sample (ΔT_s) which differs from that indicated by thermometers (ΔT_{th}). There are two kinds of detrimental temperature gradients within Cu blocks influencing ΔT_s measurements: gradients produced by heaters along the vertical axis (ΔT_{ha} and ΔT_{hb}; see Fig. 1) and those, of unknown direction, resulting from an inhomogeneous temperature distribution in the gas-flow cryostat (their horizontal components are denoted as ΔT_{ua} and ΔT_{ub}). To get rid of the vertical gradients the thermometers were fixed on these block surfaces which are adjacent to the sample. The second problem was overcame by the following compensation procedure. Two subsequent runs with two different values of ΔT_{th} were always performed (in order to make ΔT_{ua} and ΔT_{ub} reproducible we kept all possible run parameters constant, including the temperature drift rate and the gas flow rate). Then, the following formula was used to determine the actual thermopower S of the sample:

$$S = \frac{U_1}{\Delta T_{s,1}} = \frac{U_2}{\Delta T_{s,2}} = \frac{U_1 - U_2}{\Delta T_{th,1} - \Delta T_{th,2}}, \quad (1)$$

where U stands for the measured voltage and indices 1 and 2 denote the first and second runs, respectively. The validity of this approach was confirmed by several tests with $\Delta T_{th,1} \approx -\Delta T_{th,2}$ and with $\Delta T_{th,1} \neq 0$ and $\Delta T_{th,2} \approx 0$ on shorter and longer Pb samples. During the measurements on the MgB_2 single crystal we kept $\Delta T_{th,1}$ linearly varying between 0.5 K at LHe temperature and 2 K at room temperature, whereas $\Delta T_{th,2}$ was kept close to zero.

III. RESULTS

Figure 2 presents the zero-field measurements on MgB_2 single crystals performed using both equipments along the ab plane and the c axis. The differences between TEP values for different samples and for same sample mea-
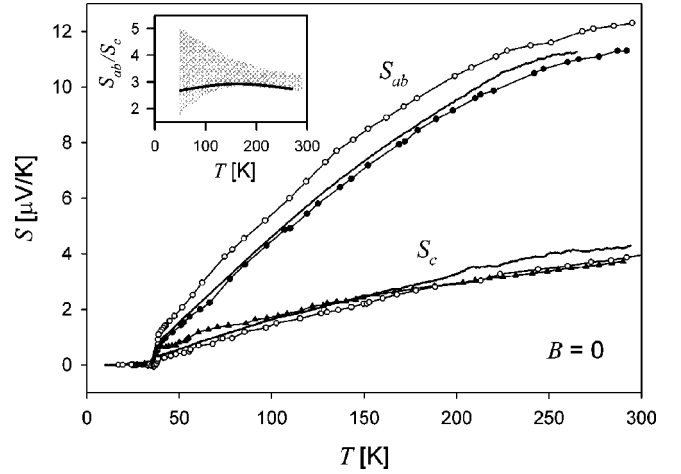

FIG. 2. Zero-field thermoelectric power measured on MgB_2 single crystals along the ab plane and the c axis. Symbols denote results obtained using the semi-automatic equipment (solid circles, sample A; open circles, sample B; solid triangles, sample C); thick solid lines denote measurements performed by the automatic equipment on sample A. The inset shows the thermopower anisotropy ratio (solid line, data for sample A by the automatic equipment; the dashed area represents the uncertainty due to the results scatter for all samples).

sured by different equipments do not exceed 10% (S_{ab}) and 13% (S_c) at room temperature and 33% (S_{ab}) and 50% (S_c) at $T = 50$ K. The higher data spread for the c axis results is caused by the particularly short length of the samples along this direction (~ 0.1 mm) what made the compensation procedure less effective.

Our TEP values for the ab plane exceed these found in a recent work[13] ($S_{ab} = 11.3$–12.3 μV/K at 293 K in our measurements versus $S_{ab} \approx 7$ μV/K measured in Ref. 13). Measurements performed on polycrystalline material revealed TEP values either close to our in-plane results[14] or, more frequently, values in the middle between S_{ab} and S_c.[13,15–21] Surprisingly, despite the fact that the c axis electrical conductivity is much lower than that for the ab plane,[7] we have found that S_c values for MgB_2 are substantially lower than the in-plane ones ($S_c \approx 3.7$–4.3 μV/K at 293 K).

The character of the TEP temperature dependence is very similar for both directions: the $S(T)$ dependence is almost linearly increasing with temperature between T_c and ~ 80 K (slope 6.2×10^{-8} V/K^2 for S_{ab} and 2.2×10^{-8} V/K^2 for S_c), at higher temperature the curvature becomes increasingly negative. This is in contrast with Ref. 13, where a wide maximum around $T \approx 60$ K was found for $S_{ab}(T)$. The inset in Fig. 2 shows the thermopower anisotropy ratio which is of the order of 3–4 in the whole temperature range.

Figure 3 presents the results of the in-field thermopower measurements for a configuration with $B \| ab$ plane $[\angle(B,ab) = 0° \pm 10°]$ and $\nabla T \| ab$ plane. Figure 3(a) shows the TEP behavior in the normal state up to $T = 100$ K. At $B = 0$ normal-state $S_{ab}(T)$ varies almost linearly, at $B = 6$ T the S_{ab} values are only slightly higher, whereas at $B = 13$ T the growth of S_{ab} is already evident (by $\sim 20\%$ at 80 K). This nonlinear field dependence of TEP was confirmed by a
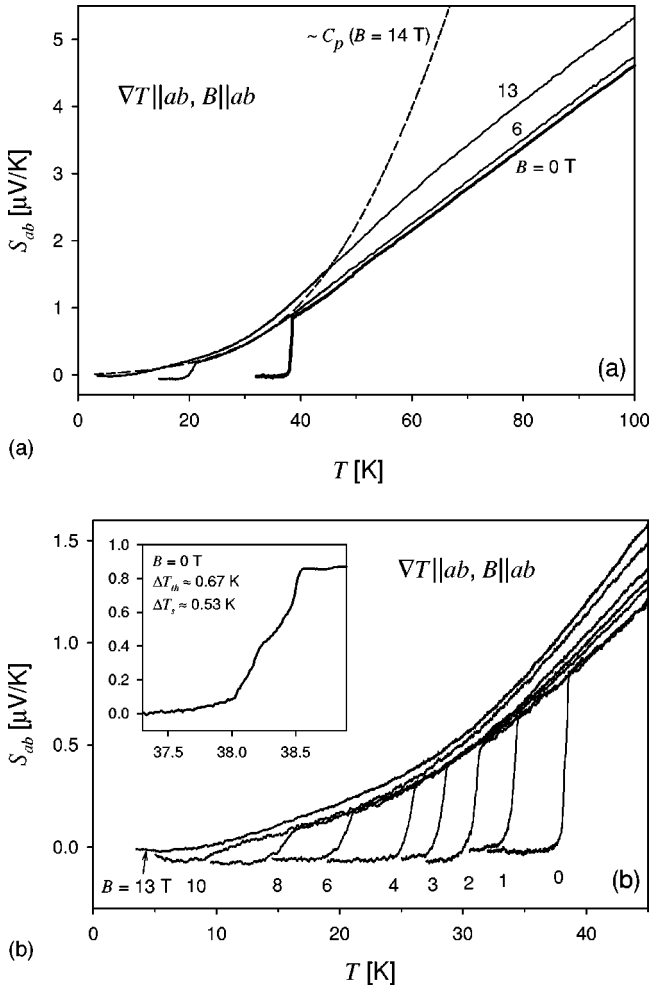
FIG. 3. Field-dependent thermoelectric power of MgB$_2$ single crystal (sample A) for $B \| \nabla T \| ab$ plane: (a) in the temperature range up to 100 K for $B = 0$, 6 and 13 T (the dashed line is proportional to the normal-state specific heat data taken from Ref. 32); (b) in the temperature range 4–45 K (the inset shows the magnified view of the superconducting transition at $B = 0$).

separate measurement of $S_{ab}(B)$ at constant temperature (not shown). Figure 3(b) presents a more detailed view of the influence of the magnetic field on the superconducting transition. In our case the field of $B = 13$ T is enough to destroy the superconductivity at all. Somewhat lower values of the B_{c2} were found here in comparison to these reported in literature (compare, e.g., Ref. 22). The reason is probably our limited accuracy in aligning the ab-plane of the crystal along the B direction. The dashed curve shows the scaling between the MgB$_2$ specific data and the thermopower, see Sec. IV for details. The inset shows the magnified view of the superconducting transition at $B = 0$. The apparent transition width of ~ 0.5 K is comparable to the estimated temperature difference across the sample $\Delta T_s = 0.53$ K (which is $\sim 20\%$ lower then the apparent temperature difference, ΔT_{th}), so that the actual transition width may be even lower.

Results for a skewed configuration $\angle(B, ab) = 30° \pm 10°$ and $\nabla T \| ab$ plane is shown in Fig. 4. Results for the normal state are very similar to that presented for the parallel con-
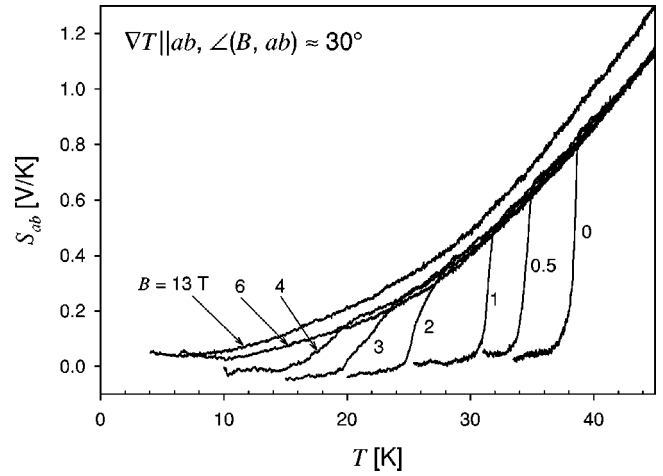

FIG. 4. Field-dependent thermoelectric power of MgB$_2$ single crystal (sample A) for a skewed configuration with $\angle(B, ab) = 30° \pm 10°$ and $\nabla T \| ab$ plane.

figuration (Fig. 3), however B_{c2} values are substantially lowered: a field of $B = 6$ T is now enough to destroy superconductivity at all.

The thermoelectric power measured for $B \| c$ axis and $\nabla T \| c$ axis is presented in Fig. 5. For this configuration the alignment of the platelet-shaped crystal in a $B \| c$ axis position is of much higher accuracy. On the other hand, extremely short length of the crystal along the c axis (~ 0.1 mm) made our compensation procedure less effective and higher absolute measurements errors should be expected. Figure 5(a) shows the $S_c(T)$ behavior in the normal state up to $T = 100$ K. For $B = 0$ $S_c(T)$ decreases almost linearly with temperature down to T_c, for $B = 6$ and 13 T $S_c(T)$ curves are linear down to ~ 60 K, then they deviates downwards. In contrast to S_{ab}, above ~ 60 K S_c increases approximately linearly with the magnetic field (by $\sim 25\%$ at 80 K for $B = 13$ T). This linear-type field dependence of TEP was confirmed by a separate measurement of $S_c(B)$ at constant temperature (not shown).

In the superconducting state TEP should drop to zero. As seen, in our case some error remained uncompensated, giving the apparent value of $S_c = +0.13$ μV/K just below T_c (this corresponds to the measured voltage of only ~ 80 nV). Therefore, we applied an additional correction using the $S_c(T, B = 0)$ line for $T < T_c$ extrapolated up to 42 K. Figure 5(b) shows the corrected S_c data in the region of the superconducting transition. The apparent transition widths are higher than for the $B \| ab$ plane configuration: $\Delta T_c \approx 2$ K for $B = 0$. Magnetic fields up to 1.2 T do not modify the shape of the normal state curve, which may be fitted by the $aT + cT^3$ formula (dashed line, see Sec. IV).

The highest field at which we detected a superconducting transition is $B = 2$ T only. However, at this field the normal-state $S_c(T)$ dependence deviates downwards from the these observed for lower fields. The tendency is more clear for the $B = 6$ T curve, for which a round, negative peak with the maximum at $T = 27$ K appears. The height of the peak increases with the field (see the curve for $B = 13$ T). The origin of the influence of the magnetic field on normal-state TEP in
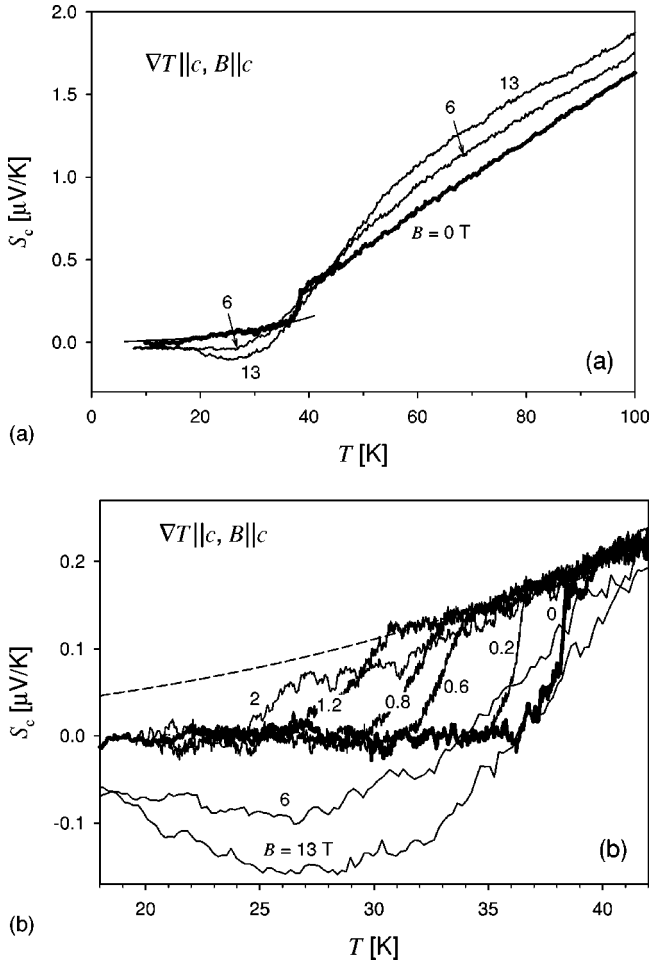
FIG. 5. Field-dependent thermoelectric power of MgB_2 single crystal (sample A) for $B\|\nabla T\|c$ axis: (a) in the temperature range up to 100 K for $B=0,6$ and 13 T, the dashed line is a fit used as a correction in Fig. 6(b); (b) the corrected data—details of the superconducting transition in the temperature range 18–42 K.

MgB_2 seems to be unclear. For pure simple metals the magneto-thermopower was accounted for the increase of the phonon-drag term [the case of noble metals, Cu, Ag, and Au (Ref. 23)] or the change of the electron-phonon enhancement leading to the increase of the diffusive TEP [the case of Al (Refs. 24 and 25)]. In the case of the complicated, highly anisotropic and multiband electronic structure of MgB_2 the explanation of the magneto-thermopower is an extremely difficult task.[26] Waiting for the larger single crystals necessary for more precise and comprehensive TEP measurement, we could only make some suggestions. If the phonon-drag term is dominating, as was proved by fitting the low temperature part of the normal-state curves, then, in the first approximation, the magnetothermopower may be tentatively attributed to the phonon-drag effects too. The main arguments are some analogies with more classical materials. That is, the positive magnetothermopower observed for MgB_2 above T_c for both directions resembles the case of the noble metals,[27] for which it was observed that the phonon-drag peak is strongly enhanced with the magnetic field. The negative peak in $S_c(T)$ appearing at $T\sim27$ K for $B>2$ T

have some similarity with a negative peak in the $S(T)$ at $T=35$ K for graphite, which is also strongly increasing with magnetic field.[28,29] This low-temperature feature was also accounted for the phonon-drag effects.

TEP data for all three measurement orientations are summarized in the phase diagram presented in Fig. 6. The critical temperature values were determined in the middle of the transition. All the $B_{c2}(T)$ lines have a slightly positive curvature. The middle curve, measured at the skewed configuration with $\angle(B,ab)=30°$ and $\nabla T\|ab$ plane, goes definitely closer to that for the out-of-plane $(B\|\nabla T\|c)$ configuration than to that for the in-plane $(B\|\nabla T\|ab)$ one. This confirms that the B_{c2} slope is determined mainly by the orientation of the magnetic field versus crystal axes, and not by the direction of the thermal gradient.
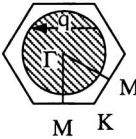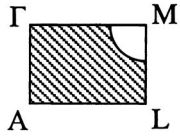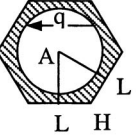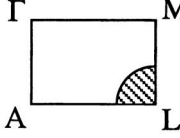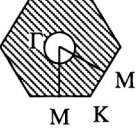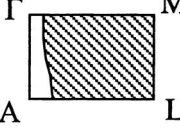
IV. DISCUSSION

A. Anisotropy

As shown by the electronic structure calculations,[5,30] the transport properties of MgB_2 are determined by contributions four sheets of the Fermi surface of comparable values of the electron density of states. Two π-type sheets are three-dimensional; the antibonding one centered at $k_z=0$ is of electron type, and the bonding one centered at $k_z=\pi/c$ is of hole type. The two similar hole-type σ sheets are almost cylindrical, with very low out-of-plane dispersion. Table I schematically shows the cross sections of the Fermi surface sheets along the two principal directions. Each of the bands contributes to the total diffusion TEP, S_d, according to the well-known expression which may be derived from the Mott formula[31]

$$S_d = -\frac{\pi^2 k_B^2 T}{3|e|}\left(\frac{\partial \ln \sigma}{\partial \varepsilon}\right)_{\varepsilon=E_F} \approx -\frac{\pi^2 k_B^2 T}{3|e|}\left(\frac{\partial \ln A_F}{\partial \varepsilon}\right)_{\varepsilon=E_F},$$

(2)

where $\sigma = \Lambda \times A_F$ is the electrical conductivity, A_F stands for the area of the Fermi surface sheet. If, as in the second part of Eq. (2) the energy dependence of the electron mean-free-path Λ is neglected, then, the sign of the TEP contribution from a particular band is determined rather by the slope of the $A_F(\varepsilon)$ dependence and not by the sign of charge carriers indicated by the sign of the Hall coefficient. A careful analysis of the electronic structure data given in Fig. 1 of Ref. 5 leads to the conclusion that the Fermi-surface sheets connected with both σ bands as well as the antibonding π band are collapsing with increasing energy, whereas the sheet connected with the bonding π band is expanding with increasing energy. Thus, the three sheets characterized by the negative value of the derivative give a positive contribution the diffusion thermopower. On the other hand, the bonding π band with positive value of the gives a negative contribution (see the first column of Table I). Therefore, for the ab plane, for which all four bands take part in the transport phenomena, the three positive diffusive TEP contributions should definitely prevail the single negative one. On the contrary, since the σ bands do not participate in the transport along the c

TABLE I. Schematics of the cross-sections of the Fermi-surface sheets for the particular bands along the two principal directions. The dashed regions represent filled states. The slope of the Fermi surface area dependence on energy $dA_F/d\varepsilon$ was estimated by the analysis of the electronic structure data given in Fig. 1 of Ref. 5. The sign of the diffusion TEP S_d was determined using Eq. (2). The sign of the phonon-drag TEP S_{ph} was determined using the Ziman rule. Namely, the electrons scattered in N-processes by phonons of quasimomentum which are crossing filled or unfilled regions of the Brillouin zone (see examples for both π band cross-sections for the ab plane) give, respectively, negative or positive contributions to S_d (Ref. 33). The sign of the Hall coefficient R_H was determined by the sign of the curvature of the respective Fermi-surface cross section.

Band	Cross-section along the ab-plane	Cross-section parallel to the c-axis
π-antibonding, centered at $k_z=0$, $dA_F/d\varepsilon<0$ $S_d=(-)\times(-)=(+)$	$S_{ph}=(-)$ $R_H=(-)$	$S_{ph}=(+)$ $R_H=(+)$
π-bonding, centered at $k_z=\pi/c$, $dA_F/d\varepsilon>0$ $S_d=(-)\times(+)=(-)$	$S_{ph}=(+)$ $R_H=(+)$	$S_{ph}=(-)$ $R_H=(-)$
two σ-bands $dA_F/d\varepsilon<0$ $S_d=(-)\times(-)=(+)$	$S_{ph}=(+)$ $R_H=(+)$	do not contribute
	net values: $S_d=(+)(-)(+)(+)\approx2(+)$ $S_{ph}=(-)(+)(+)(+)\approx2(+)$ $R_H=(-)(+)(+)(+)\approx2(+)$	net values: $S_d=(+)(-)\approx0$ $S_{ph}=(-)(+)\approx0$ $R_H=(-)(+)\approx0$

axis, the two mutually opposite contributions of the π bands are expected to roughly cancel each other making the absolute value of S_c much smaller than S_{ab}. The sign of S_c cannot be estimated (see the last row of Table I). The results of the above analysis seem to agree with the observed results of the TEP anisotropy, for which $0<S_c<S_{ab}$ was found.

Despite this qualitative agreement we have also to consider the phonon-drag TEP, S_{ph}. That is, since the Debye temperature of MgB$_2$ is particularly high $[\Theta_{eff}=920$ K at $T=298$ K (Ref. 32)] S_{ph} may play an important role even near the room temperature (a maximum of S_{ph} could be expected at $T\approx\Theta_{eff}/5=184$ K). The estimation of the signs of the phonon-drag TEP contributions of particular bands may be performed according to the Ziman rule.[33] Specifically, for the convex Fermi-surface sheets (which is the case, compare Fig. 3 in Ref. 5) and considering only scattering in N processes a negative phonon-drag TEP is anticipated for the electron bands and a positive one for the hole bands. For the ab plane this gives three positive contributions (from both σ bands and from the bonding π band) and a single negative one (from the antibonding π band). The net value is again positive, as in the case of the diffusion TEP (it is interesting to indicate that for both π bands S_d and S_{ph} are of opposite

signs). Now, we consider the phonon-drag TEP for the c axis. The σ bands do not contribute. Due to a honeycomb structure of both π bands the curvature of the cross-section along the c axis is opposite to that of the cross-section parallel to the ab plane (i.e., S_{ph} is positive for the antibonding π band and negative for the bonding π band). Thus, both π bands S_{ph} contributions again roughly cancel each other resulting in the low absolute value of S_c predicted for this direction, the same as in the analysis of the diffusive TEP.

A similar analysis may be also used for the Hall coefficient, in this case the sign is determined by the curvature of the Fermi-surface cross-section perpendicular to the magnetic field. The sign prediction for R_H for particular bands exactly agree with these for the phonon-drag TEP (see Table I), thus giving a large, positive net result for the ab plane and smaller, undetermined in sign result for the c axis. These predictions could be compared with the resent measurements of the R_H anisotropy described in Ref. 7. In accordance with our predictions, the authors found the in-plane Hall coefficient positive ($R_{Hxy}=+160\times10^{-12}$ m^3/C at room temperature), whereas the out-of-plane coefficient was found smaller in absolute value and negative ($R_{Hxz}=R_{Hzx}=-40\times10^{-12}$ m^3/C at room temperature).
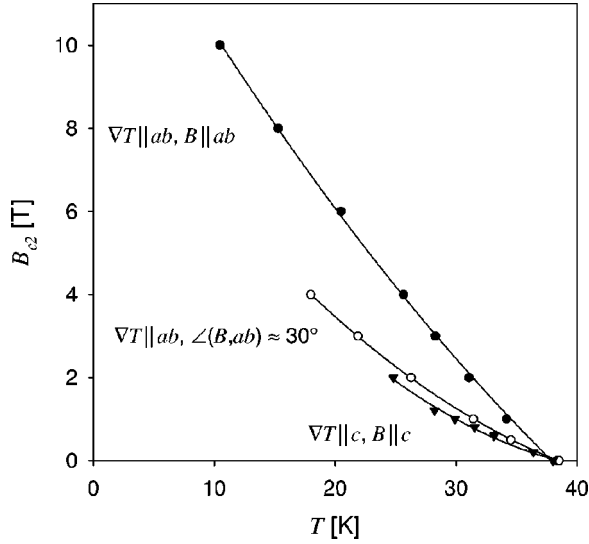
FIG. 6. Superconducting phase diagram of single-crystal MgB_2 derived from TEP measurements at three orientations: $B \| \nabla T \| ab$, $B \| \nabla T \| c$ and a skewed one, with $\angle (B,ab) = 30°$ and $\nabla T \| ab$.

Summarizing, the analysis of the Fermi surface topology leads to the conclusion that S_{ab} should be relatively large and positive, whereas the absolute value of Sc is expected to be much smaller than S_{ab} due to the interplay between the two π bands, giving mutually opposite contributions both in case of S_d and S_{ph} (the sign of S_c remained undetermined in the above analysis). This agrees well with our experimental results. A further support of the presented physical picture was given by the Hall effect analysis. However, the above picture is not able to indicate the dominating mechanism contributing to the thermopower: the diffusive or the phonon-drag one (this problem will be addressed in Sec. IV B).

B. Low temperature analysis

The diffusive and phonon-drag TEP are strictly connected with electronic (C_e) and phonon (C_L) specific heat, respectively. In low temperature approximations ($T \ll \Theta_D$) these relations may be expressed by following simple formulas:[31]

$$S_d = \frac{2 C_e}{3ne}, \tag{3}$$

$$S_{ph} = r \frac{C_L}{3ne}, \tag{4}$$

where n is the charge carrier concentration and r is the phonon-electron coupling parameter defined by the ratio of the phonon-electron scattering rate to the total of phonon scattering rates. Thus, $r \approx 1$ in case of dominating phonon-electron scattering and $0 < r < 1$ if other phonon scattering processes are important.

Therefore, for the total TEP at low temperature a simple dependence is expected:
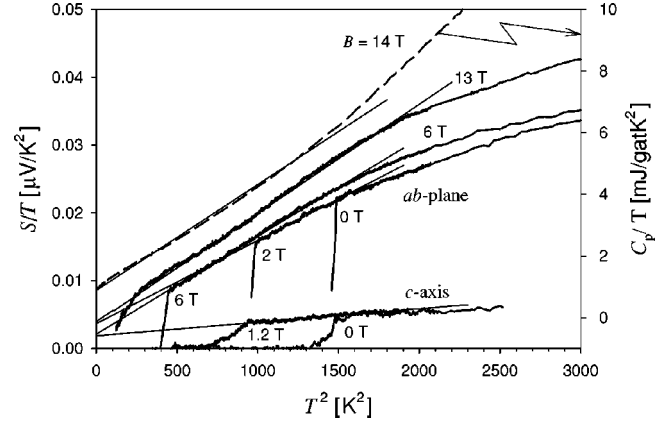
$$S = aT + cT^3. \tag{5}$$

FIG. 7. S/T (thick solid lines) and C_p/T (dashed line, data taken from Ref. 32) as a function of T^2; the solid thin lines are fits according to Eq. (5) for TEP and to the $C_p = \gamma T + \beta T^3$ relation for specific heat for $T < 40$ K.

The a and c coefficients are connected with the Sommerfeld coefficient γ ($C_e = \gamma T$) and the β coefficient describing the low temperature behavior of the lattice specific heat ($C_L = \beta T^3$) through the following relations:

$$a = \frac{2 \gamma}{3 n_{fu} N_A e} \tag{6}$$

$$c = r \frac{\beta}{3 n_{fu} N_A e}, \tag{7}$$

where n_{fu} is the carrier concentration per formula unit and N_A is the Avogadro number. Despite the complicated nature of MgB_2 electronic structure the simple formula given by Eq. (5) is fulfilled for $T \lesssim T_c$ (compare dashed lines in Figs. 3 and 5). To perform more quantitative evaluation of that scaling we plotted S/T and C_p/T versus T^2 (see Fig. 7). From the specific heat data below $T \sim 40$ K the values of $\gamma = 8.9 \times 10^{-4}$ J/gat K^2 and $\beta = 3.4 \times 10^{-6}$ J/gat K^4 have been found. Due to the multiband nature of the MgB_2 the Hall effect cannot be used for the estimation of n_{fu}. Therefore, one should rather use the results of the band structure calculations which predict that the total n_{fu} is of the order of unity.[27,34] Thus, just to get an idea on the order of magnitude of the quantities of interest we assumed $n_{fu} = 1$ for the present estimations.

Table II presents the a and c coefficients calculated using Eqs. (6) and (7) as well as the fitting parameters for TEP. As seen, the a and c values derived from $C_p(T)$ agree well in the order of magnitude with these obtained from $S_{ab}(T)$, supporting the validity of the physical picture used. Moreover, similar values of c parameters indicate that the phonon-electron coupling for the ab plane is $r_{ab} \approx 1$. Another conclusion is that at low temperature the phonon-drag contribution dominates the total S_{ab} of MgB_2. For example, at $T = 40$ K the S_{ph}/S_d ratio estimations vary between 5 and 11. This result stands in opposition with the previous interpretations of the TEP behavior, which attributed the dominating role rather to the diffusive TEP.[13,18] Similar fitting procedure performed by authors of Ref. 18 above T_c in a higher

TABLE II. The coefficients for the linear (a) and cubic (c) terms describing the low temperature dependence of TEP as well as the ratio of the phonon-drag and diffusive TEP contributions, S_{ph}/S_d, at 40 K. The data scatter for the ab plane results from both the measurements errors and the influence of the magnetic field.

data origin	a (mV/K^2)	c (mV/K^4)	S_{ph}/S_d at 40 K
specific heat [Eqs. (6) and (7)]	6.1×10^{-3}	1.2×10^{-5}	3.1
S_{ab} at $B=13$ T	4.0×10^{-3}	1.6×10^{-5}	6
$B=6$ T	2.1×10^{-3}	1.5×10^{-5}	11
$B=2$ T	3.7×10^{-3}	1.2×10^{-5}	5
S_c for $B\leqslant1.2$ T	1.9×10^{-3}	2.0×10^{-6}	1.7

temperature range 45–90 K gave the values $a=1.76\times10^{-2}$ mV/K^2 and $c=1.26\times10^{-6}$ mV/K^4, and, thus, the S_{ph}/S_d ratio was found as small as 0.11 at $T=40$ K.

For the c axis, the a parameter (describing the diffusive TEP) is nearly of the same value as that found for S_{ab}, whereas the c parameter (describing the phonon-drag TEP) is one order of magnitude smaller in comparison to its in-plane counterpart. Hence, the S_{ph}/S_d ratio was found equal only to 1.7 at $T=40$ K. This means that at low temperature the electron-phonon coupling for the c axis, r_c, is much lower than this for the ab plane direction:

$$\frac{r_{ab}}{r_c}=\frac{c_{ab}}{c_c}=7\pm1. \qquad (8)$$

This conclusion, which is the central one for the current paper, agrees well with that given in the report on the de Haas–van Alphen effect.[35] The authors have found that the electron-phonon coupling strength λ (defined as the electron mass enhancement factor) is a factor ~3 larger on the two-dimensional (2D) σ orbits than on the 3D π orbits.

At higher temperature S_{ph} deviates from the scaling with C_L due to increasing role of the phonon-phonon scattering, thus reducing the r parameter. For simple metals a maximum at $\Theta_D/5$ is usually observed. Such a feature was not found for MgB$_2$ (it would be expected at $T\approx\Theta_{eff}/5=184$ K), both for S_{ab} and S_c. Instead, a saturation tendency is observed (see Fig. 2).

Due to the scatter of obtained a and c parameters the above analysis cannot support or falsify our suggestions (see Sec. III), that the positive magneto-thermopower found for both directions above T_c should be accounted for in terms of the phonon-drag effects.

V. SUMMARY

In the present report we describe the thermoelectric power measurements of the MgB$_2$ single crystals performed in the temperature range 4–300 K and in the magnetic field up to $B=13$ T. Three configurations were studied: with $B\|\nabla T\|ab$ (in-plane), with $B\|\nabla T\|c$ (out-of-plane) and with $\angle(B,ab)=30°$ and $\nabla T\|ab$ plane (skewed configuration).

Both the in-plane and the out-of-plane zero-field thermopower was found positive, with similar, metal-like behavior and the anisotropy ratio S_{ab}/S_c of the order of 3–4 in the whole temperature range. Low values of the S_c are surprising in the face of the high electrical resistivity along the c axis reported in the literature.[7] This paradox was qualitatively explained in terms of the Fermi surface topology. It was shown that total TEP of the contributions from particular sheets of the Fermi surface is large and positive for the in-plane direction, whereas for the c axis it should be much lower in absolute value (the sign of Sc remained undetermined).

The low temperature ($T\leqslant40$ K), normal-state thermopower measured in the magnetic field was analyzed in terms of a sum of two contributions: a linear one arising from the diffusive TEP and a cubic one connected with the phonon-drag TEP. A scaling with the literature data on normal-state specific heat[32] supported this approach. This analysis indicated a dominant role of the phonon-drag thermopower in comparison to the diffusive one, especially for the ab plane (at 40 K the ratio S_{ph}/S_d is of the order of 5–11 for the ab plane and ~2 for the c axis). A comparison of the phonon-drag contributions for both directions gave an evidence for a strong (by a factor of $\sim7\pm1$) anisotropy of the electron-phonon coupling. The positive magneto-thermopower found above T_c for both directions as well as the negative feature in $S_c(T)$ at $T\sim27$ K for $B>2$ T were also tentatively attributed to phonon-drag effects.

*Email address: T.Plackowski@int.pan.wroc.pl

[1] J. Nagamatsu, N. Nakagawa, T. Muranaka, Y. Zenitani, and J. Akimitsu, Nature (London) **410**, 63 (2001).

[2] H. Uchiyama, S. Tajima, K.M. Shen, D.H. Lu, and Z.-X. Shen, Physica C **385**, 85 (2003).

[3] D.G. Hinks and J.D. Jorgensen, Physica C **385**, 98 (2003).

[4] H. Kotegawa, K. Ishida, Y. Kitaoka, T. Muranaka, and J. Akimitsu, Phys. Rev. Lett. **87**, 127001 (2001).

[5] I.I. Mazin and V.P. Antropov, Physica C **385**, 49 (2003).

[6] R.A. Riberio, S.L. Bud'ko, C. Petrovic, and P.C. Canfield, Physica C **385**, 16 (2003).

[7] Yu. Eltsev, K. Nakao, S. Lee, T. Masui, N. Chikumoto, S. Tajima, N. Koshizuka, and M. Murakami, Phys. Rev. B **66**, 180504(R) (2002).

[8] J. Karpinski, S.M. Kazakov, J. Jun, M. Angst, R. Puźniak, A. Wiśniewski, and P. Bordet, Physica C **385**, 42 (2003).

[9] R.B. Roberts, Philos. Mag. **36**, 91 (1977).

[10] F.J. Blatt, A.D. Caplin, C.K. Chiang, and P.A. Schroeder, Solid State Commun. **15**, 411 (1974).

[11] E.R. Rumbo, J. Phys. F: Met. Phys. **6**, 85 (1976).

[12] E.L. Christenson, J. Appl. Phys. **34**, 1485 (1963).

[13] T. Masui, K. Yoshida, S. Lee, A. Yamammoto, and S. Tajima, Phys. Rev. B **65**, 214513 (2002).

[14] J.S. Ahn, E.S. Choi, W. Kang, D.J. Singh, M. Han, and E.J. Choi,

Phys. Rev. B **65**, 214534 (2002).

[15] W. Liu, J. Huang, Y. Wang, X. Wang, Q. Feng, and A. Yan, Solid State Commun. **118**, 575 (2001).

[16] T. Muranaka, J. Akimitsu, and M. Sera, Phys. Rev. B **64**, 020505(R) (2001).

[17] B. Lorenz, R.L. Meng, Y.Y. Xue, and C.W. Chu, Phys. Rev. B **64**, 052513 (2001).

[18] M. Putti, E. Galleani d'Agliano, D. Marre, F. Napoli, M. Tassisto, P. Manfrinetti, and A. Palenzona, in *Studies of High Temperature Superconductors*, edited by A. Narlikar (Nova, New York, 2001), Vol. 38.

[19] M. Schneider, D. Lipp, A. Gladun, P. Zahn, A. Handstein, G. Fuchs, S.-L. Drechsler, M. Richter, K.-H. Müller, and H. Rosner, Physica C **363**, 6 (2001).

[20] B. Fisher, K.B. Chashka, L. Patlagan, and G.M. Reisner, Physica C **384**, 10 (2003).

[21] D.C. Kim, J.S. Kim, B.H. Kim, Y.W. Park, C.U. Jung, and S.I. Lee, Physica C **387**, 313 (2003).

[22] U. Welp, A. Rydh, G. Karapetrov, W.K. Kwok, G.W. Crabtree, C. Marcenat, L.M. Paulius, L. Lyard, T. Klein, J. Marcus, S. Blanchard, P. Samuely, P. Szabo, A.G.M. Jansen, K.H.P. Kim, C.U. Jung, H.-S. Lee, B. Kang, and S.-I. Lee, Physica C **385**, 154 (2003).

[23] F.J. Blatt, A.D. Caplin, C.K. Chiang, and P.A. Schroeder, Solid State Commun. **15**, 411 (1974).

[24] B.J. Thaler and J. Bass, J. Phys. F: Met. Phys. **6**, 2315 (1976).

[25] J.L. Opsal and D.K. Wagner, J. Phys. F: Met. Phys. **6**, 2323 (1976).

[26] K. Yagasaki and A.T. Burkov, in *Encyclopedia of Materials: Science and Technology*, edited by K.H.J. Buschow, R.W. Cahn, M.C. Flemings, B. Ilschner, E.J. Kramer, and S. Mahajan (Elsevier, Amsterdam, 2001), pp. 4757–4761.

[27] J.M. An and W.E. Pickett, Phys. Rev. Lett. **86**, 4366 (2001).

[28] K. Sugihara, T. Takezawa, T. Tsuzuku, Y. Hishiyama, and A. Ono, J. Phys. Chem. Solids **33**, 1475 (1972).

[29] A. Ono and Y. Hishiyama, Philos. Mag. **59**, 271 (1989).

[30] V.G. Kogan and S.L. Bud'ko, Physica C **385**, 131 (2003).

[31] F.J. Blatt, P.A. Schroeder, C.L. Foiles, and D. Greig, *Thermoelectric Power of Metals* (Plenum Press, New York, 1976).

[32] Y. Wang, T. Plackowski, and A. Junod, Physica C **355**, 179 (2001).

[33] J.M. Ziman, Adv. Phys. **10**, 1 (1961).

[34] P.P. Singh, Phys. Rev. Lett. **87**, 087004 (2001).

[35] J.R. Cooper, A. Carrington, P.J. Meeson, E.A. Yelland, N.E. Hussey, L. Balicas, S. Tajima, S. Lee, S.M. Kazakov, and J. Karpinski, Physica C **385**, 75 (2003).